Coordinated Science Laboratory

UNIVERSITY OF ILLINOIS - URBANA, ILLINOIS

PASSIVE DAMPING OF THE GENERAL RELATIVITY SATELLITE GYRO

T.C. Chen , J. Hsu , D. Skaperdas

REPORT R-330 NOVEMBER , 1966

THis work was supported in part by the Joint Services Electronics Program (U.S. Army, U.S. Navy, and U.S. Air Force) under Contract DA 28 043 AMC 00073(E); and in part by the NASA NGR 14 005 038.

CORRECTED ACKNOWLEDGEMENT PAGE FOR R-330

This work was supported in part by the Joint Services Electronics Program (U.S. Army, U.S. Navy, and U.S. Air Force) under Contract DA 28 043 AMC 00073: and in part by the NASA NsG-443.

Abstract

A passive damping method for aligning the instantaneous spin, symmetry and angular momentum axes of a solid, axially symmetric almost spherical satellite gyro is analyzed. Damping is accomplished by the dissipation of energy due to cyclic strains in the gyro body caused by its torque-free precession. Damping time is calculated for a particular gyro design.

PASSIVE DAMPING OF THE GENERAL
RELATIVITY SATELLITE GYRO

1. Damping Mechanics of Precessing Body

The demands on a gyro spin axis readout system based on a preferred moment of inertia axis are simplified if the gyro symmetry axis $\underline{\omega}_3$, angular momentum vector $\underline{h}$ and instantaneous spin axis $\underline{\omega}$ are colinear. In general, when a spinning gyro is suddenly released in free fall, these three axes will not be colinear as shown in Fig. 1, resulting in a torque-free motion of the gyro about its angular momentum vector.[1] Even if these axes were colinear, an environmental disturbance such as a micrometeorite collision could cause cratering, thereby shifting the symmetry axis with respect to the angular momentum axis,[2] resulting in a torque-free motion. For an axially symmetric gyro this motion is a steady precession of its instantaneous spin axis $\underline{\omega}$ and symmetry axis $\underline{\omega}_3$ about its angular momentum axis $\underline{h}$, as shown in Fig. 2 from the point of view of an observer fixed in inertial space. In this figure the outer cone (body cone), whose axis is $\underline{\omega}_3$, rolls without slipping on the inner cone (space cone), whose axis is $\underline{h}$, and the line of intersection is the instantaneous spin axis $\underline{\omega}$. This precession of the symmetry axis $\underline{\omega}_3$ about $\underline{h}$ complicates the readout problem; consequently, a damping mechanism which aligns the three axes within a reasonable time is required. This report analyzes a passive damping scheme in which energy is dissipated by virtue of cyclic strains in the gyro body caused by its torque-free precession.[3] The gyro will be considered an axially symmetric solid, spherical in shape except for two diametrically opposite flats, which give a preferred moment-of-inertia C (polar). The moment of inertia about the perpendicular axis is A. The case for a thin, spherical shell has been analyzed.[4,4a]

The analysis of the combined effects of gravity gradient, centrifugal distortion and the statistics of micrometeorite cratering leads to an optimum gyro diameter of about one foot.[5] For a gyro of this diameter the analysis of micrometeorite cratering[6] gives a relationship between the number of hits per year, each of which could cause an angular disturbance of 0.6 arc sec per year, versus (C-A)/C. For one hit per year the ratio $(C-A)/C \approx .01$. Assuming a Poisson distribution for the meteorite flux, this gives a probability of 0.92 for having one month of undisturbed data. It is important, then, that the damping time be quite smaller than one month in order to separate the effects of such cratering from the spin axis orientation data.

The quantities $\underline{\omega}_3$, $\underline{h}$, and $\underline{\omega}$ in Fig. 1 are coplaner, and the angles θ and α are related by[1]

$$\tan \theta = \frac{A}{C} \tan \alpha \qquad (1\text{-}1)$$

so that if A = C, then $\underline{h}$ and $\underline{\omega}$ become colinear and $\underline{\omega}_3$ loses its significance. For (C-A)/C = .01 the angle ϵ between $\underline{h}$ and $\underline{\omega}$ will be small and is given approximately as $\epsilon \approx [(C-A)/C] \tan \alpha$. For example, if $\alpha = 0.4$ degrees, $\epsilon \approx 14$ arc sec. During initial gyro spinup attempts will be made to keep α as small as possible, but there will be some misalignment error. The maximum allowable error is determined by the tolerance within which the satellite spin axis must lie in its orbital plane, which is of the order of 0.4 degrees for the present gyro parameters.[5] This means that $\underline{\omega}_3$ must be known with respect to the gyro body to better than 0.4 degrees.

For axially symmetric bodies the rate $\dot{\Psi}$ at which $\underline{\omega}_3$ and $\underline{\omega}$ precess about $\underline{h}$ for the case of free precession (zero torque) is given by[1]

$$\dot{\Psi} = \frac{C}{A-C} \frac{\dot{\phi}}{\cos\theta} \tag{1-2}$$

where θ is the angle between $\underline{\omega}_3$ and $\underline{h}$. The quantity $\dot{\phi}$, (later referred to as the elastic vibrating frequency) is the angular rate at which the $\underline{\omega}$ vector moves about the body as viewed by an observer stationed on the body. Therefore, if the spinning body is centrifugally distorted, an observer stationed along $\underline{\omega}_3$ will see the body undergo periodic deformation at a fundamental rate $\dot{\phi}$ corresponding to the rotation rate of the $\underline{\omega}$ vector about the observer. This is shown rigorously in Section 3. Equation (1-2) can be rewritten with the aid of Fig. 3, which shows the geometrical relation of the involved quantities. Since $\omega_o = \dot{\Psi} + \dot{\phi}/\cos\theta$ eliminating $\dot{\Psi}$ gives

$$\dot{\phi} = \frac{A-C}{A} \omega_o \cos\theta \tag{1-3}$$

where $\underline{\omega}_o$ is the initial gyro satellite angular velocity.

The periodic deformation of an anelastic body gives rise to a rate of energy dissipation which, among other things, depends upon the fraction of the elastic energy which is dissipated in each deformation or strain cycle.[3] This fraction, γ, is called the hysteretic damping factor, and is a measure of the internal friction of the anelastic body. Metallurgists who measure internal friction usually state results in terms of logarithmic decrement D, quality factor Q, or angle δ by which strain lags stress.[7] The logarithmic decrement is the logarithm to the base e of two successive amplitudes of a freely oscillating body. The various factors which measure internal friction are related as follows, for $Q > 10$:

$$Q = \frac{2\pi}{\gamma} = \frac{\pi}{D} = \tan\delta \ . \tag{1-4}$$

The effect of internal energy dissipation is to decrease the angle θ between the symmetry axis $\underline{\omega}_3$ and $\underline{h}$, which is shown as follows. The kinetic energy T of the axially symmetric body in Fig. 1 can be written as

$$T = \frac{1}{2} A({\omega_1}^2 + {\omega_2}^2) + \frac{1}{2} C{\omega_3}^2 \ . \tag{1-5}$$

Also,

$$\begin{aligned} \underline{h} &= \hat{i}A\omega_1 + \hat{j}A\omega_2 + \hat{k}C\omega_3 \\ \underline{h}\cdot\underline{h} &= h^2 = A^2({\omega_1}^2 + {\omega_2}^2) + C^2{\omega_3}^2 \ . \end{aligned} \tag{1-6}$$

Multiply Eq. (1-5) by 2A and subtract from Eq. (1-6) to get $h^2 - 2AT = C(C-A)\omega_3{}^2$.

Since $C\omega_3 = C\omega_o \cos\theta = h\cos\theta$, solving for T gives

$$T = \frac{h^2}{2A}\left[1 - \left(\frac{C-A}{C}\right)\cos^2\theta\right].$$

For a finite dissipation, with constant $\underline{h}$, the time rate of change of kinetic energy is

$$\dot{T} = \frac{h^2}{A}\left(\frac{C-A}{C}\right)\cos\theta\ \sin\theta\ \dot{\theta}\,. \tag{1-7}$$

For the case $C > A$, and for a negative value of $\dot{T}$ (energy dissipation), $d\theta/dt$ is negative; therefore, θ decreases.

It is shown later that the total gyro elastic strain energy can be classified into two parts. The first part is independent of $\dot{\phi}$ and is represented as a dc or constant term. Strictly speaking, it is dependent upon θ and $\dot{\theta}$ and hence slowly changing with time, but this change is negligible compared with the second part. The second part of the elastic strain energy varies with time at a rate $\dot{\phi}$, and all higher harmonics of $\dot{\phi}$ up to the fourth. It is this time varying part which is responsible for the hysteretic damping of precession. If we call W that portion of the gyro elastic strain energy per cycle of stress (whose fundamental frequency is $\dot{\phi}$), then the fraction of this energy which is dissipated per cycle of stress is γW and the rate of dissipation is $\gamma W\dot{\phi}/2\pi$. This must be equal to the rate of decrease in kinetic energy $\dot{T}$ as given by Eq. (1-7). We then have

$$\dot{W} = \frac{\gamma W \dot{\phi}}{2\pi} = -\dot{T} .$$

Substituting $\dot{\phi}$ from Eq. (1-3), letting $h = C\omega_o$ and solving for $\dot{\theta}$, one obtains

$$\dot{\theta} = \frac{\gamma W}{2\pi \; C\omega_o \; \sin\theta} . \tag{1-8}$$

Sections 2 and 3 describe the method of determining W for a solid, spherical body with preferred moment-of-inertia axis C, such that $C/A \approx 1.01$. There it will be shown that W is a function of gyro radius a, gyro material, spin speed ω_o and angle θ as in the following equation for small values of θ.

$$W = \frac{4\pi^2 \rho^2 \omega_o^4 a^7 \theta^2}{E} \Gamma \tag{1-9}$$

where Γ is a dimensionless quantity which is a function of gyro geometry and material. Substituting this into Eq. (1-8), with $\sin\theta \approx \theta$ and $C \approx (2/5)Ma^2 = (8/15)\pi a^5 \rho$ gives

$$\dot{\theta} = \frac{15}{4E} \gamma \rho \omega_o^3 a^2 \Gamma \theta . \tag{1-10}$$

The solution of (1-10) for the damping time t for an initial angle θ_i and a final angle θ_f is

$$t = \frac{4E}{15 \; \gamma \rho \omega_o^3 a^2 \; \Gamma} \mathrm{Ln} \left(\frac{\theta_f}{\theta_i} \right) . \tag{1-11}$$

It remains to determine Γ, which is obtained from the strain energy W for a rotating solid sphere in torque-free precession.

2. Inertia Force Field

Consider a solid sphere rotating about an instantaneous axis $\underline{\omega}$ as in Fig. 3. The instantaneous axis of rotation $\underline{\omega}$ is misaligned with the angular momentum vector $\underline{h}$ due to some disturbance which has also shifted the symmetry axis $\underline{\omega}_3$ from the momentum axis $\underline{h}$ by a small angle θ according to Eq. (1-1). If $\dot{\theta}$ is assumed to be small in comparison with the spin velocity $\dot{\phi}$ and the precession $\dot{\Psi}$, then the angular velocity $\underline{\omega}$ can be written as

$$\underline{\omega} = \hat{i}\dot{\Psi}\ \sin\theta\cos\phi + \hat{j}\dot{\Psi}\ \sin\theta\sin\phi + \hat{k}(\dot{\phi}+\dot{\Psi}\ \cos\theta) \qquad (2\text{-}1)$$

where θ, Ψ, ϕ are Euler angles defining the orientation of the body axes x,y,z with respect to the space axes X,Y,Z as shown in Fig. 4 and $\hat{i}$, $\hat{j}$, $\hat{k}$ are unit vectors along the axes x, y, z respectively. The angular acceleration $\dot{\underline{\omega}}$ is

$$\dot{\underline{\omega}} = \frac{\partial \omega}{\partial t} + \underline{\omega} \times \underline{\omega}\ .$$

Assuming that θ, $\dot{\phi}$ and $\dot{\Psi}$ are constant,

$$\dot{\underline{\omega}} = \dot{\phi}\dot{\Psi}\ \sin\theta(-\ \hat{i}\ \sin\phi + \hat{j}\ \cos\phi)\ .$$

Substituting (2-1) and (2-2) into the equation for linear acceleration

$$\underline{a} = \underline{a}_o + \underline{a}' + \underline{\omega} \times (\underline{\omega} \times \underline{r}) + \underline{\dot{\omega}} \times \underline{r} + 2\underline{\omega} \times \underline{v}' \tag{2-3}$$

and noting the following approximations[1,3]

$$\underline{a}_o = \underline{a}' = \underline{v}' = 0 \tag{2-4}$$

$$\begin{aligned}
\underline{a} = \omega_o^2 \hat{i}\Big[&-x\left(\cos^2\theta + \frac{C^2}{A^2}\sin^2\theta\sin^2\phi\right) + y\left(\frac{C}{A}\right)^2 \sin^2\theta\sin\phi\cos\phi \\
&+ z\left(\frac{C}{A}\right)\sin\theta\cos\theta\cos\phi + z\left(1 - \frac{C}{A}\right)\frac{C}{A}\sin\theta\cos\theta\cos\phi\Big] \\
&+ \omega_o^2 \hat{j}\Big[x\,\frac{C^2}{A^2}\sin^2\theta\sin\phi\cos\phi - y\left(\cos^2\theta + \frac{C^2}{A^2}\sin^2\theta\cos^2\phi\right) \\
&+ z\,\frac{C}{A}\sin\theta\cos\theta\sin\phi + z\left(1 - \frac{C}{A}\right)\frac{C}{A}\sin\theta\cos\theta\sin\phi\Big] \\
&+ \omega_o^2 \hat{k}\Big[x\,\frac{C}{A}\sin\theta\cos\theta\cos\phi + y\,\frac{C}{A}\sin\theta\cos\theta\sin\phi - z\,\frac{C^2}{A^2}\sin^2\theta \\
&- x\left(1 - \frac{C}{A}\right)\frac{C}{A}\sin\theta\cos\theta\cos\phi + y\left(1 - \frac{C}{A}\right)\frac{C}{A}\sin\theta\cos\theta\sin\phi\Big].
\end{aligned} \tag{2-5}$$

Under the assumption that $\dot{\theta}$ is negligible compared with $\dot{\phi}$ and $\dot{\Psi}$, the only time-varying quantity in (2-5) is $\phi = \dot{\phi}t$ and the inertia force varies harmonically at a rate $\dot{\phi}$ and $2\dot{\phi}$ as can be seen from the above equation.

If it is assumed that the body can be approximated by a homogeneous sphere so that the ratio $\frac{C}{A}$ is equal to unity, then the above acceleration becomes

$$\underline{a} = \hat{i}\omega_o^2\Big[-x(\cos^2\theta + \sin^2\theta\sin^2\phi) + y\ \sin^2\theta\sin\phi\cos\phi + z\ \sin\theta\cos\theta\cos\phi\Big]$$

$$+ \hat{j}\omega_o^2\Big[x\ \sin^2\theta\sin\phi\cos\phi - y(\cos^2\theta + \sin^2\theta\cos^2\phi) + z\ \sin\theta\cos\theta\sin\phi\Big]$$

$$+ \hat{k}\omega_o^2\Big[x\ \sin\theta\cos\theta\cos\phi + y\ \sin\theta\cos\theta\sin\phi - z\ \sin^2\theta\Big]. \tag{2-6}$$

The problem is now reduced to finding the displacement field in a sphere subjected to an inertia force $\underline{F} = -\rho\ \underline{a}$.

A general method of solution for a sphere subjected to body force was given by Chree[8] who, as an example, has worked out the displacement field of a sphere rotating about a diametric axis. In that case the problem becomes axisymmetric but such a symmetry is lost when the body force field is that due to acceleration (2-6) which takes into account the influence of precession of the spin axis. In the following, a brief account of Chree's method and its application to the present non-axisymmetric case will be given.

3. Displacement Field in a Sphere Subjected to Inertia Force

Chree's method mentioned above is essentially based on the existence of a body force potential which is expanded in spherical harmonics. Consider Navier's equation of equilibrium

$$(\lambda+\mu)\nabla\nabla\cdot\underline{u} + \mu\nabla^2\underline{u} + \rho\underline{F} = 0$$

where λ and μ are Lame's constants, $\underline{u}$ is the displacement and $\underline{F}$ is the inertia force per unit mass due to the acceleration $\underline{a}(= -\underline{F}/\rho)$

expressed by (2-6). This may be written in indicial notation as

$$(\lambda+\mu)\Delta,_{i} + \mu u_{i,kk} + \rho F_{i} = 0 \qquad (3\text{-}1)$$

$\Delta \equiv \nabla\cdot\underline{u}$ is the dilatation, $P,_{i} \equiv \frac{\partial P}{\partial x_{i}}$, $i \equiv 1,2,3$ for any function P and the triad x,y,z becomes x_1, x_2, x_3. If F_i and u_i are derivable from potentials V_n (an $n^{\underline{th}}$ order spherical harmonic) and Φ, respectively, such that

$$F_{i} = V_{n,i}$$

$$u_{i} = \Phi,_{i} \qquad (3\text{-}2)$$

then (3-1) becomes

$$(\lambda+\mu)\Phi,_{kk} + \rho V_{n} = 0 \; . \qquad (3\text{-}3)$$

Because of the identity

$$(r^{m}V_{n}),_{kk} = m(m + 2n + 1)r^{m-2}\, V_{n} \qquad (3\text{-}4)$$

where m and n are positive integers, Eq. (3-4) is satisfied by

$$\Phi = - \frac{\rho}{2(\lambda+2\mu)\,(2n+3)}\, r^{2}\, V_{n}. \qquad (3\text{-}5)$$

The displacement field corresponding to this Φ is, from (3-6) and (3-3),

$$u_{i} = - \frac{\rho}{2(\lambda+2\mu)\,(2n+3)}\, (r^{2}\, V_{n}),_{i} \qquad (3\text{-}6)$$

which is accompanied by a surface traction

$$T_i = -\frac{\rho\mu}{r(\lambda+2\mu)}\left[\frac{n+1}{2n+3}\, r^2 V_{n,i} + \left\{\frac{\lambda}{\mu} + \frac{2(n+1)}{2n+3}\right\} x_i V_n\right] \tag{3-7}$$

across any spherical surface r = constant. If a body is bounded by the surface r = a where the surface traction is zero, the displacement u_i is determined by adding to (3-6) the displacements corresponding to ω- and Φ-type solutions.[9] This yields surface tractions

$$\frac{rT_i}{\mu} = (2n+\alpha_n)r^2\omega_{n,i} + \left[2n\left(\frac{\lambda}{\mu} + 1\right) + \alpha\left\{(n+3)\,\frac{\lambda}{\mu} + (n+2)\right\}\right] x_i\omega_n$$

$$\alpha_n = -2\,\frac{n\lambda + (3n+1)\mu}{(n+3)\lambda + (n+5)\mu} \tag{3-8}$$

and

$$\frac{rT_i}{\mu} = 2(n-1)\Phi_{n,i} \tag{3-9}$$

respectively, where, in this case, ω_n and Φ_n are to be taken as

$$\omega_n = \rho B_1 V_n$$

$$\Phi_n = \rho B_2 V_n \; . \tag{3-10}$$

For the case $T_i = 0$ on $r = a$, these constants B_1 and B_2 are given by

$$B_1 = \frac{\left\{(2n+3)\lambda + (2n+2)\mu\right\}\left\{(n+3)\lambda + (n+5)\mu\right\}}{2(2n+3)(\lambda+2\mu)\mu\left\{(2n^2+4n+3)\lambda + 2(n^2+n+1)\mu\right\}} \tag{3-11}$$

$$B_2 = \frac{n\left\{(n+2)\lambda + (n+1)\mu\right\}a^2}{2(n-1)\mu\left\{(2n^2+4n+3)\lambda + 2(n^2+n+1)\mu\right\}}$$

where n is the order of the spherical harmonic, V_n.

It can be shown easily that the inertia force field due to (2-6) is derivable from the potential

$$V = r^2 V_o + V_2 \tag{3-12}$$

where V_o and V_2 are spherical harmonics of zeroth and second order given by

$$V_o = \frac{\omega_o^2}{3} \quad \text{and} \tag{3-13a}$$

$$\begin{aligned} V_2 = {} & \frac{\omega_o^2}{6}(3\cos^2\theta + 3\sin^2\theta\sin^2\phi - 2)x^2 \\ & + \frac{\omega_o^2}{6}(3\cos^2\theta + 3\sin^2\theta\cos^2\phi - 2)y^2 \\ & + \frac{\omega_o^2}{6}(3\sin^2\theta - 2)z^2 + \\ & - \omega_o^2 \sin^2\theta\sin\phi\cos\phi\, xy \\ & - \omega_o^2 \sin\theta\cos\theta\sin\phi\, yz \\ & - \omega_o^2 \sin\theta\cos\theta\cos\phi\, xz\ . \end{aligned} \tag{3-13b}$$

It is interesting to note that the potential given by (3-12) and (3-13) reduces, as it should, to that of a spinning sphere given by Chree[8] when the misalignment θ is set to zero.

By substituting (3-12) into (3-6) and superposing the displacements due to ω_n- and Φ_n-type potentials given by (3-10) and (3-11) to ensure the satisfaction of the boundary condition on $r = a$, after considerable amount of algebra, one obtains the following expressions for the components of the displacement.

$$u_1 = \left[\frac{\rho\,\omega_o{}^2 a^2 (5\lambda+6\mu)}{15(\lambda+2\mu)(3\lambda+2\mu)} - \frac{2B_2}{3}\,\omega_o{}^2 + B_2\omega_o{}^2\,\cos^2\theta + B_2\omega_o{}^2\,\sin^2\theta\,\sin^2\phi\right]x$$

$$- \left[B_2\omega_o{}^2\,\sin^2\theta\,\sin\phi\,\cos\phi\right]y - \left[B_2\omega_o{}^2\,\sin\theta\,\cos\theta\,\cos\phi\right]z$$

$$+ \left[\left\{-\frac{2}{3}B_1 + \frac{1}{35}L + \frac{B_1 M}{3}\right\}\omega_o{}^2\right.$$

$$+ \left\{B_1 - \frac{1}{7}L - \frac{B_1}{2}M\right\}\omega_o{}^2\,\cos^2\theta$$

$$\left. + \left\{B_1 - \frac{1}{7}L - \frac{B_1}{2}M\right\}\omega_o{}^2\,\sin^2\theta\,\sin^2\phi\right]x^3$$

$$+ \left[-B_1 + \frac{1}{14}L\right]\omega_o{}^2\,\sin^2\theta\,\sin\phi\,\cos\phi\;\;y^3$$

$$+ \left[-B_1 + \frac{1}{14}L\right]\omega_o{}^2\,\sin\theta\,\cos\theta\,\cos\phi\;\;z^3$$

$$+ \left[-B_1 + \frac{3}{14}L + B_1 M\right]\omega_o{}^2\,\sin^2\theta\,\sin\phi\,\cos\phi\;\;x^2 y$$

$$+\left[-B_1+\frac{3}{14}L+B_1M\right]\omega_o^{\,2}\sin\theta\cos\theta\cos\phi\;x^2z$$

$$+\left[\left\{-\frac{2}{3}B_1+\frac{1}{35}L+\frac{B_1}{3}M\right\}\omega_o^{\,2}\right.$$

$$+\left\{B_1-\frac{1}{7}L-\frac{B_1}{2}M\right\}\omega_o^{\,2}\cos^2\theta-\left\{\frac{1}{14}L\right\}\omega_o^{\,2}\sin^2\theta$$

$$\left.+\left\{B_1-\frac{B_1}{2}M\right\}\omega_o^{\,2}\sin^2\theta\cos^2\phi\right]y^2x$$

$$+\left[-B_1+\frac{1}{14}L\right]\omega_o^{\,2}\sin^2\theta\cos\theta\cos\phi\;y^2z$$

$$+\left[\left\{-\frac{2}{3}B_1-\frac{3}{70}L+\frac{B_1}{3}M\right\}\omega_o^{\,2}+B_1\omega_o^{\,2}\cos^2\theta-\frac{B_1}{2}M\,\omega_o^{\,2}\sin^2\theta\right.$$

$$\left.+\left\{B_1-\frac{1}{14}L\right\}\omega_o^{\,2}\sin^2\theta\sin^2\phi\right]z^2x$$

$$+\left[-B_1+\frac{1}{14}L\right]\omega_o^{\,2}\sin^2\theta\sin\phi\cos\phi\;z^2y$$

$$+\left[\frac{1}{7}L+B_1M\right]\omega_o^{\,2}\sin\theta\cos\theta\sin\phi\;xyz\;. \tag{3-14a}$$

$$u_2=-B_2\omega_o^{\,2}\sin^2\theta\sin\phi\cos\phi\;x\;.$$

$$+\left[\left\{-\frac{2}{3}B_2+\frac{\rho\,a^2(5\lambda+6\mu)}{15(\lambda+2\mu)(3\lambda+2\mu)}\right\}\omega_o^{\,2}+B_2\omega_o^{\,2}\cos^2\theta\right.$$

$$+ B_2\omega_o^{\,2} \sin^2\theta \cos^2\phi \Big] y - B_2\omega_o^{\,2} \sin\theta \cos\theta \sin\phi \; z$$

$$+ \left[- B_1 + \frac{1}{14} L\right] \omega_o^{\,2} \sin^2\theta \sin\phi \cos\phi \; x^3$$

$$+ \Bigg[\left\{- \frac{2}{3} B_1 + \frac{1}{35} L + \frac{B_1}{3} M\right\} \omega_o^{\,2} + \left\{B_1 - \frac{1}{7} L - \frac{B_1}{2} M\right\} \omega_o^{\,2} \cos^2\theta$$

$$+ \left\{B_1 - \frac{1}{7} L - \frac{B_1}{2} M\right\} \omega_o^{\,2} \sin^2\theta \cos^2\phi \Bigg] y^3 + \left[-B_1 + \frac{1}{14} L\right] \times$$

$$\omega_o^{\,2} \sin\theta \cos\theta \sin\phi \; z^3$$

$$+ \Bigg[\left\{- \frac{2}{3} B_1 + \frac{1}{35} L + \frac{B_1}{3} M\right\} \omega_o^{\,2} + \left\{B_1 - \frac{1}{7} L - \frac{B_1}{2} M\right\} \omega_o^{\,2} \cos^2\theta$$

$$- \frac{1}{14} L \, \omega_o^{\,2} \sin^2\theta$$

$$+ \left\{B_1 - \frac{B_1}{2} M\right\} \omega_o^{\,2} \sin^2\theta \sin^2\phi \Bigg] x^2 y$$

$$+ \left[-B_1 + \frac{1}{14} L\right] \omega_o^{\,2} \sin\theta \cos\theta \sin\phi \; x^2 z$$

$$+ \left[-B_1 + \frac{3}{14} L + B_1 M\right] \omega_o^{\,2} \sin^2\theta \sin\phi \cos\phi \; y^2 x$$

$$+ \left[-B_1 + \frac{3}{14} L + B_1 M\right] \omega_o^{\,2} \sin\theta \cos\theta \sin\phi \; y^2 z$$

$$+ \left[-B_1 + \frac{1}{14} L\right] \omega_o^{\,2} \sin^2\theta \sin\phi \cos\phi \; z^2 x$$

$$+ \left[\left\{ - \frac{2}{3} B_1 - \frac{3}{70} L + \frac{B_1}{3} \right\} \omega_o^{\;2} + B_1 \omega_o^{\;2} \cos^2\theta \right.$$

$$\left. + \left\{ B_1 - \frac{1}{14} L \right\} \omega_o^{\;2} \sin^2\theta \cos^2\phi \right] z^2 y$$

$$+ \left[\frac{1}{7} L + B_1 M \right] \omega_o^{\;2} \sin\theta \cos\theta \cos\phi \; xyz \; . \qquad \text{(3-14b)}$$

$$u_3 = - B_2 \omega_o^{\;2} \sin\theta \cos\theta \cos\phi \; x - B_2 \omega_o^{\;2} \sin\theta \cos\theta \sin\phi \; y$$

$$+ \left[\left\{ \frac{B_2}{3} + \frac{\rho a^2 (5\lambda+6\mu)}{15(\lambda+2\mu)(3\lambda+2\mu)} \right\} \omega_o^{\;2} - B_2 \omega_o^{\;2} \cos^2\theta \right] z$$

$$+ \left[-B_1 + \frac{1}{14} L \right] \omega_o^{\;2} \sin\theta \cos\theta \cos\phi \; x^3 + \left[-B_1 + \frac{1}{14} L \right] \times$$

$$\omega_o^{\;2} \sin\theta \cos\theta \sin\phi \; y^3$$

$$+ \left[\left\{ - \frac{12}{15} L + \frac{B_1}{3} M \right\} \omega_o^{\;2} + \left\{ \frac{1}{7} L - B_1 M \right\} \omega_o^{\;2} \cos^2\theta \right] z^3$$

$$+ \left[- B_1 + \frac{1}{14} L \right] \omega_o^{\;2} \sin\theta \cos\theta \sin\phi \; x^2 y$$

$$+ \left[\left\{ \frac{B_1}{3} - \frac{3}{70} L + \frac{B_1}{3} M \right\} \omega_o^{\;2} - \left\{ B_1 + \frac{B_1}{2} M \right\} \omega_o^{\;2} \cos^2\theta \right.$$

$$\left. - \left\{ \frac{1}{14} L + \frac{B_1}{2} M \right\} \omega_o^{\;2} \sin^2\theta \sin^2\phi \right] x^2 z$$

$$+ \left[B_1 + \frac{1}{14} L \right] \omega_o^{\,2} \sin\theta \cos\theta \cos\phi \quad y^2 x$$

$$+ \left[\left\{ \frac{B_1}{3} - \frac{3}{70} L + \frac{B_1}{3} M \right\} \omega_o^{\,2} - \left\{ B_1 + \frac{B_1}{2} M \right\} \omega_o^{\,2} \cos^2\theta \right.$$

$$\left. - \left\{ \frac{1}{14} L + \frac{B_1}{2} M \right\} \omega_o^{\,2} \sin^2\theta \cos^2\phi \right] y^2 z$$

$$+ \left[-B_1 + \frac{3}{14} L + B_1 M \right] \omega_o^{\,2} \sin\theta \cos\theta \cos\phi \quad z^2 x$$

$$+ \left[-B_1 + \frac{3}{14} L + B_1 M \right] \omega_o^{\,2} \sin\theta \cos\theta \sin\phi \quad z^2 y$$

$$+ \left[\frac{1}{7} L + B_1 M \right] \omega_o^{\,2} \sin\theta \sin\phi \cos\phi \quad xyz \, . \tag{3-14c}$$

where

$$L = \frac{1}{\lambda + 2\mu}$$

$$M = \frac{4\lambda + 14\mu}{5\lambda + 7\mu} \, . \tag{3-15}$$

Terms in these components of displacement can be classified into three categories, the first group being the steady part which does not depend on ϕ at all, the second those which vary with time at a rate $\dot{\phi}$, and lastly those which pulsate at a rate $2\dot{\phi}$. The last two categories which vary with time are responsible for the hysteretic damping of precession.

4. Elastic Strain Energy of Solid Sphere

The time varying part of the elastic strain energy can be computed by first taking one half the dot product of the force field $-\rho\underline{a}$, where $\underline{a}$ is given by (2-6), and the displacement field $\underline{u}$, given by (3-15), to give the strain energy density W' such that

$$W' = \frac{1}{2}(-\rho a_i)u_i \tag{4-1}$$

and then dropping all the steady terms which are independent of ϕ. The amount of alternating strain energy W per cycle of precession is

$$W = \int_o^{2\pi} \int_\Omega W' \, d\Omega \, d\phi \tag{4-2}$$

where Ω is the volume of the sphere. By substituting (2-6) and (3-14) into (4-1) and (4-2), and dropping terms of the order of $\sin^4\theta$ in comparison with those proportional to $\sin^2\theta$, it is not hard, although tedius, to obtain

$$W = 4\pi^2\rho^2\omega_o^4 a^7\theta^2 \left\{ \frac{B_2}{5a^2} + \frac{20}{63} B_1 - \frac{9}{980} L - \frac{19}{630} B_1 M \right\} \tag{4-3}$$

as the fundamental component of the alternating part of elastic strain energy per unit cycle of precession. Designating the quantity within brackets as Γ', one has

$$\Gamma' = \frac{B_2}{5a^2} + \frac{20B_1}{63} - \frac{9}{980} L - \frac{19}{630} B_1 M . \tag{4-4}$$

Equation (4-4) may be simplified by first substituting λ and μ into the expressions for L and M of (3-15) and B_1 and B_2 of (3-11), to get

$$L = \frac{(1+\nu)(1-2\nu)}{E(1-\nu)}$$

$$M = \frac{2(7+10\nu)}{7-4\nu} ,$$

and

$$B_1 = \frac{-(3+\nu)(7-4\nu)(1+\nu)}{7E(1-\nu)(7+5\nu)}$$

$$B_2 = \frac{(3+2\nu)(1+\nu)a^2}{E(7+5\nu)}$$

for n = 2.

These values of L, M, B_1 and B_2 are substituted into (4-4) to get

$$\Gamma' = \frac{1+\nu}{E}\left\{ \frac{3+2\nu}{5(7+5\nu)} - \frac{9(1-2\nu)}{980(1-\nu)} + \frac{(3+\nu)(7-4\nu)}{(1-\nu)(7+5\nu)}\left[\frac{19(7-10\nu)}{2205(7-4\nu)} - \frac{20}{441}\right]\right\}$$

$$= \frac{\Gamma}{E} \qquad (4\text{-}5)$$

which is now only in terms of Poisson's ratio ν and Young's modulus E. Equation (4-3) may be rewritten as

$$W = 4\pi^2\rho^2\omega_o^4 a^7\theta^2 \ \frac{\Gamma}{E}$$

where Γ is a function of ν only. This value of Γ, substituted in (1-11) determines the damping time t for a given gyro.

5. Numerical Calculations

The expression for damping time (1-11) may be rewritten in the form

$$t = \frac{4}{15} \frac{E}{\gamma\omega_o \Gamma(\rho\omega_o^2 a^2)} \text{ Ln}\left(\frac{\theta_f}{\theta_i}\right) \tag{5-1}$$

From elasticity theory, the maximum stress at the center of a solid, spinning sphere is approximately given by[8]

$$\sigma_{max} = \rho\omega_o^2 a^2 \left(\frac{3 + 2\nu}{7 + 5\nu}\right) \tag{5-2}$$

where ν is Poisson's ratio. Hence, the term $\rho\omega_o^2 a^2$ in the denominator of (5-1) is proportional to the maximum allowable stress for the selected gyro material. Since the optimization study referred to in Section 1 fixes the value of a to be approximately six inches, ω_o for a given material follows from equation (5-2), giving due allowance for a safety factor.

Volume electrical resistivity requirements severely restrict the choice of materials to those between the good conductors ($\rho > 10^3$ ohm cm) and good insulators ($\rho < 10^{10}$ ohm cm). The materials germanium, silicon and titanium dioxide, when properly doped, and certain glasses are among those which appear to satisfy the electrical resistivity requirements. At present, the hysteretic damping factor γ has been obtained only for certain glasses. Among other things,

$1/Q$ is a function of the elastic vibrating frequency $\dot{\phi}$ given by equation (1-3). Present gyro parameters indicate a vibration frequency of about 1 to 3 cps. Fortunately, glass has a maximum value for $1/Q(= \gamma/2\pi)$ of about 4×10^{-3} in this range of frequencies[7,11,12] at room temperature. This makes it a promising high damping factor material.

In order to determine experimentally the approximate value of σ_{max}, thin glass disks were spun to the bursting point in a motor-driven test fixture. For such disks, the maximum stress is also at the center and is, to good approximation

$$\sigma_{max} = \rho\omega^2 a^2 \left(\frac{3 + \nu}{8}\right). \tag{5-3}$$

For glass, $\nu \approx 0.16$ so that the bracketed factors in (5-2) and (5-3) become 0.425 and 0.395 for the sphere and disk, respectively. Hence, the maximum stresses are nearly the same for identical materials, diameters, and spin speed, therefore justitying the use of disks for this test. These tests indicated an upper value of ω_o of about 630 rad/sec for plate glass, with an adequate safety factor. For $C/A = 1.01$ and θ of the order of half degree, the elastic vibrating frequency $\dot{\phi}$ is about one cps, as seen from equation (1-3).

Using glass as the gyro material, the following parameters have been determined:

$$\gamma = \frac{2\pi}{Q} = .025$$

$$\rho = 2.5 \times 10^3 \text{ kgm/m}^2$$

$$\omega_o = 630 \text{ rad/sec}$$

$$a = 7.5 \text{ cm} = .075 \text{ m}$$

$$\theta_f = 0.1 \text{ arc sec}$$

$$\theta_i = 0.5 \text{ degree}$$

$$E = 7 \times 10^{10} \text{ newtons/m}^2$$

$$\nu = 0.16 \quad .$$

The value of Γ from equation (4-5) becomes $\Gamma = -0.071$. Substituting this and the above values into equation (1-11), the damping time t becomes 8.2 hrs, a reasonable time.

6. Conclusion

Using glass as a possible gyro material, the passive damping method for aligning the gyro instantaneous spin axis, angular momentum axis and symmetry axis has been shown to be feasible, requiring about 8¼ hours to damp from $\theta = 0.5$ degree to $\theta = 0.1$ arc sec. The damping time constant $\tau = 0.83$ hours. This value of damping time is probably required only during the initial gyro spin up. The statistics of micrometeorite collisions with this gyro show that there will be a probability of 0.92 for no collisions within the period of one month which could cause an angular disturbance of 0.6 arc sec per year. The effect of such a collision, however, would require only (0.83) (1.8) = 1.5 hours, a reasonable time.

7. Acknowledgments

The authors would like to acknowledge the assistance of Naren Mehta and Carl Sutton in carrying out many of the calculations, and the helpful discussions with R. D. Palamara of Purdue University.

BIBLIOGRAPHY

1. Thomson, W. T., "Introduction to Space Dynamics," Wiley, N.Y., 1961, pp. 113-117.

2. Barthel, H. O., "Effects of Micrometeoroid Cratering on the Direction of the Axis of Maximum Moment of Inertia," CSL Report R-274, Coord. Science Lab., Univ. of Illinois, Urbana, Ill., Feb. 1966.

3. Thomson, W. T., and Reiter, G. S., "Altitude Drift of Space Vehicles," J. Astronaut. Sci., 7, 29-34 (1960).

4. Palamara, R. D., "Synthesis of a General Relativity Experiment," Ph.D. thesis, Engineering Mechanics Dept., Wayne State Univ., Detroit, Mich., (1964).

5. CSL Progress Report for Dec. 1965, Jan. and Feb. 1966, Coord. Science Lab., Univ. of Illinois, Urbana, Ill.

6. Barthel, H. O., loc. cit., p. 6, Fig. 1

7. Zener, C., "Elasticity and Anelasticity of Metals," Univ. of Chicago press, Chicago, 1948, p. 60 ff.

8. Chree, C., Cambridge Phil. Soc. Trans., Vol. 14, Part 3, (1889), p. 292.

9. Love, A. E. H., "A Treatise on Mathematical Theory of Elasticity," Dover Publications, N.Y., 4th ed. pp. 250-252.

10. Bennewitz, K. and Rötger, H., "Über die Innere Reibung fester Körper; Absorptionsfrequenz von Metallen in akustischen Gebiet," Phys. Zeits chr., 37, 578 (1936).

11. Forry, K. E., "Two Peaks in the Internal Friction as a Function of Temperature in Some Soda Silicate Glasses," Am. Ceram. Soc., 40, [3], 90-94 (1957).

12. CSL report to appear.

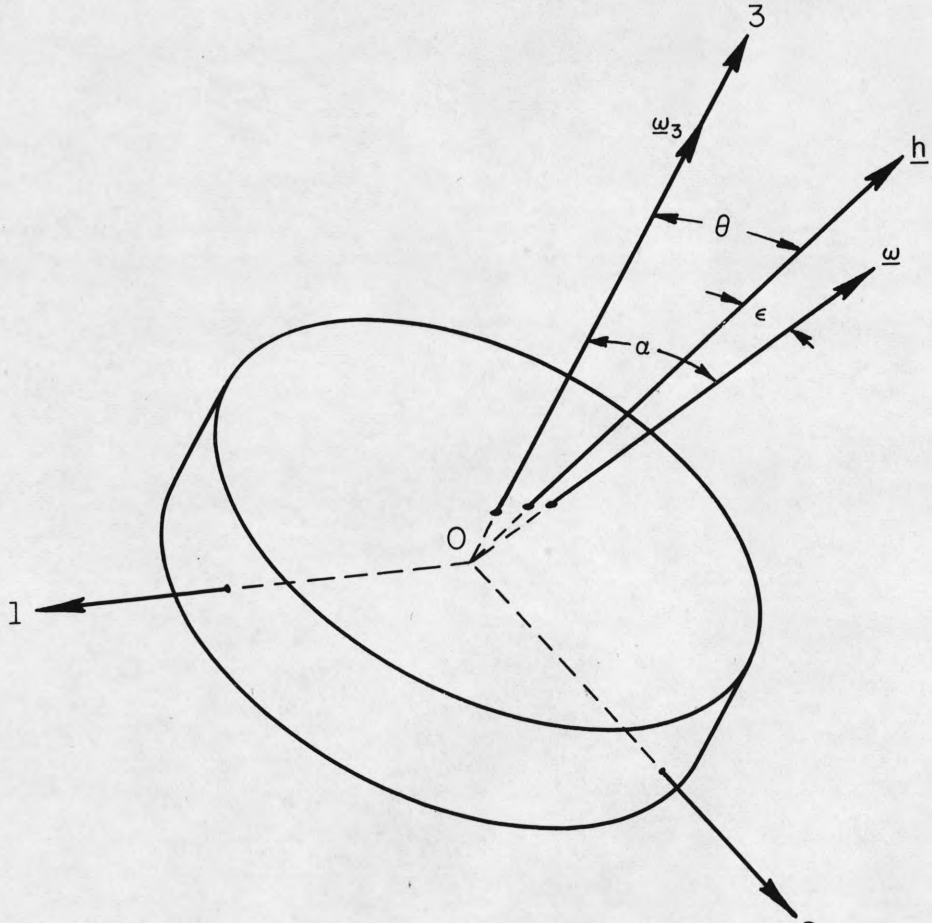

Figure 1.

RR-229

General Relationship of Angular Momentum, Symmetry and Instantaneous Spin Axes of Axially Symmetric Gyro.

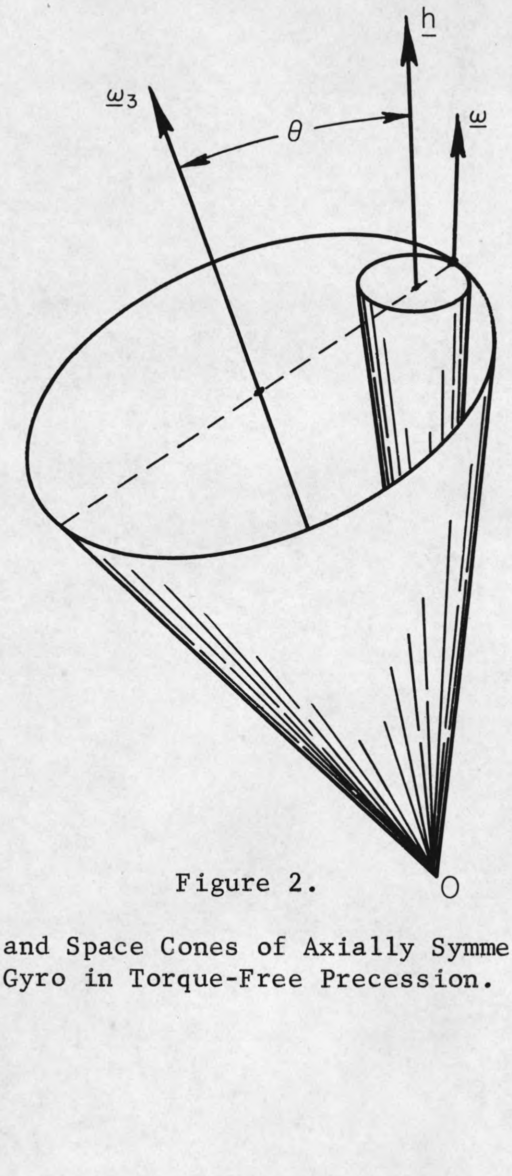

Figure 2.

RR-229

Body and Space Cones of Axially Symmetric
Gyro in Torque-Free Precession.

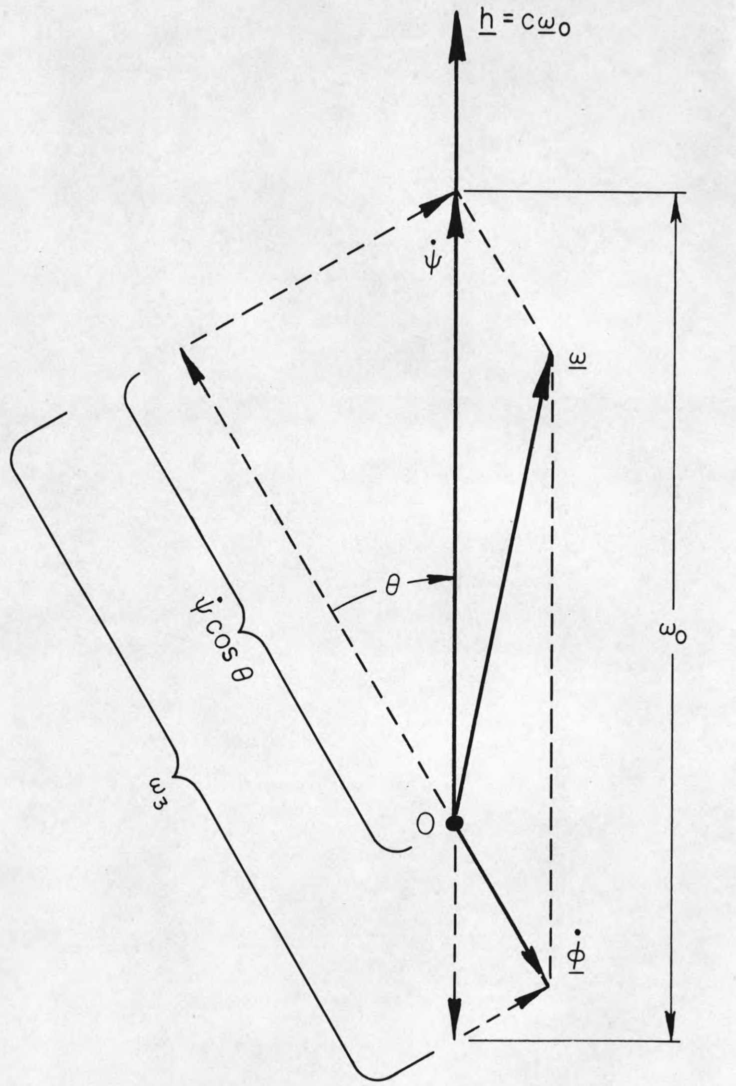

$$\omega_3 = \dot{\Psi}\cos\theta + \dot{\phi}$$

$$\overline{\omega} = \overline{\dot{\phi}} + \overline{\dot{\Psi}}$$

$$\omega_o = \dot{\Psi} + \dot{\phi}/\cos\theta$$

Figure 3.

Angular Velocity Relationships of Axially-Symmetric Gyro in Torque-Free Precession.

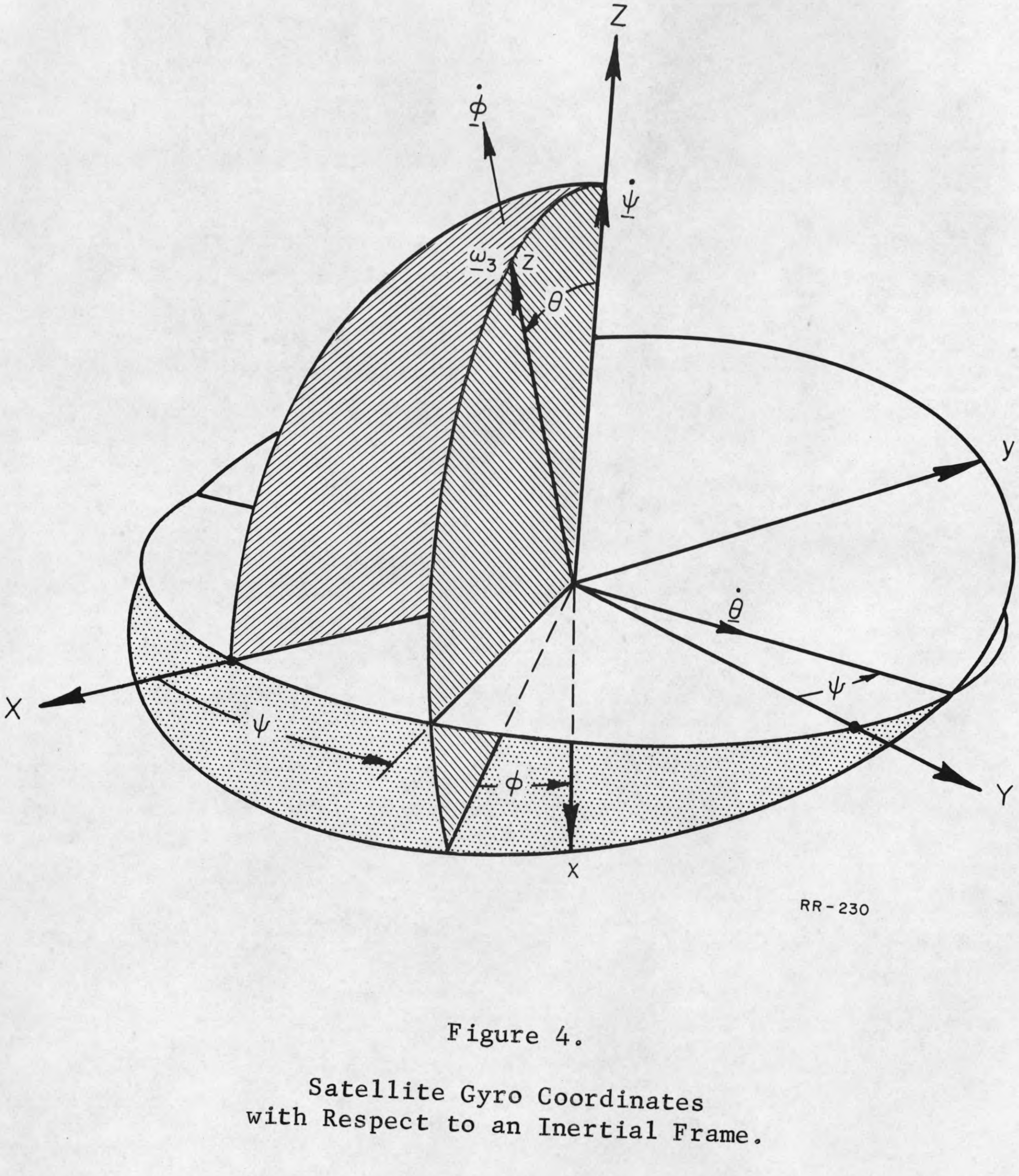

Figure 4.

Satellite Gyro Coordinates
with Respect to an Inertial Frame.

Distribution list as of May 1, 1966

1 Dr. Edward M. Reilley
Asst. Director (Research)
Ofc. of Defense Res. & Engrg.
Department of Defense
Washington, D. C. 20301

1 Office of Deputy Director
(Research and Information Rm 3D1037)
Department of Defense
The Pentagon
Washington, D. C. 20301

1 Director
Advanced Research Projects Agency
Department of Defense
Washington, D. C. 20301

1 Director for Materials Sciences
Advanced Research Projects Agency
Department of Defense
Washington, D. C. 20301

1 Headquarters
Defense Communications Agency (333)
The Pentagon
Washington, D. C. 20305

20 Defense Documentation Center
Attn: TISIA
Cameron Station, Building 5
Alexandria, Virginia 22314

1 Director
National Security Agency
Attn: Librarian C-332
Fort George G. Meade, Maryland 20755

1 Weapons Systems Evaluation Group
Attn: Col. Finis G. Johnson
Department of Defense
Washington, D. C. 20305

1 National Security Agency
Attn: R4-James Tippet
Office of Research
Fort George G. Meade, Maryland 20755

1 Central Intelligence Agency
Attn: OCR/DD Publications
Washington, D. C. 20505

1 AFRSTE
Hqs. USAF
Room 1D-429, The Pentagon
Washington, D. C. 20330

1 AUL3T-9663
Maxwell Air Force Base, Alabama 36112

1 AFFTC (FTBPP-2)
Technical Library
Edwards AFB, California 93523

1 Space Systems Division
Air Force Systems Command
Los Angeles Air Force Station
Los Angeles, California 90045
Attn: SSSD

1 SSD(SSTRT/Lt. Starbuck)
AFUPO
Los Angeles, California 90045

1 Det. #6, OAR (LOOAR)
Air Force Unit Post Office
Los Angeles, California 90045

1 Systems Engineering Group (RTD)
Technical Information Reference Branch
Attn. SEPIR
Directorate of Engineering Standards
& Technical Information
Wright-Patterson AFB, Ohio 45433

1 ARL (ARIY)
Wright-Patterson AFB, Ohio 45433

1 AFAL (AVT)
Wright-Patterson AFB, Ohio 45433

1 AFAL (AVTE/R. D. Larson)
Wright-Patterson AFB, Ohio 45433

1 Office of Research Analyses
Attn: Technical Library Branch
Holloman AFB, New Mexico 88330

2 Commanding General
Attn: STEWS-WS-VT
White Sands Missile Range
New Mexico 88002

1 RADC (EMLAL-I)
Griffiss AFB, New York 13442
Attn: Documents Library

1 Academy Library (DFSLB)
U. S. Air Force Academy
Colorado 80840

1 FJSRL
USAF Academy, Colorado 80840

1 APGC (PGBPS-12)
Eglin AFB, Florida 32542

1 AFETR Technical Library
(ETV, MU-135)
Patrick AFB, Florida 32925

1 AFETR (ETLLG-I)
STINFO Officer (for Library)
Patrick AFB, Florida 32925

1 AFCRL (CRMXLR)
AFCRL Research Library, Stop 29
L. G. Hanscom Field
Bedford, Massachusetts 01731

2 ESD (ESTI)
L. G. Hanscom Field
Bedford, Massachusetts 01731

1 AEDC (ARO, INC)
Attn: Library/Documents
Arnold AFS, Tennessee 37389

2 European Office of Aerospace Research
Shell Building
47 Rue Cantersteen
Brussels, Belgium

5 Lt. Col. E. P. Gaines, Jr.
Chief, Electronics Division
Directorate of Engineering Sciences
Air Force Office of Scientific Research
Washington, D. C. 20333

1 U. S. Army Research Office
Attn. Physical Sciences Division
3045 Columbia Pike
Arlington, Virginia 22204

1 Research Plans Office
U. S. Army Research Office
3045 Columbia Pike
Arlington, Virginia 22204

1 Commanding General
U. S. Army Materiel Command
Attn: AMCRD-RS-PE-E
Washington, D. C. 20315

1 Commanding General
U. S. Army Strategic Communications Command
Washington, D. C. 20315

1 Commanding Officer
U. S. Army Materials Research Agency
Watertown Arsenal
Watertown, Massachusetts 02172

1 Commanding Officer
U. S. Army Ballistics Research Laboratory
Attn: V. W. Richards
Aberdeen Proving Ground
Aberdeen, Maryland 21005

1 Commandant
U. S. Army Air Defense School
Attn: Missile Sciences Division C&S Dept.
P. O. Box 9390
Fort Bliss, Texas 79916

1 Commanding General
U. S. Army Missile Command
Attn: Technical Library
Redstone Arsenal, Alabama 35809

1 Commanding General
Frankford Arsenal
Attn: SMUFA-L6000 (Dr. Sidney Ross)
Philadelphia, Pennsylvania 19137

1 U. S. Army Munitions Command
Attn: Technical Information Branch
Picatinney Arsenal
Dover, New Jersey 07801

1 Commanding Officer
Harry Diamond Laboratories
Attn: Mr. Berthold Altman
Connecticut Avenue & Van Ness Street N. W.
Washington, D. C. 20438

1 Commanding Officer
U. S. Army Security Agency
Arlington Hall
Arlington, Virginia 22212

1 Commanding Officer
U. S. Army Limited War Laboratory
Attn: Technical Director
Aberdeen Proving Ground
Aberdeen, Maryland 21005

1 Commanding Officer
Human Engineering Laboratories
Aberdeen Proving Ground, Maryland 21005

1 Director
U. S. Army Engineer Geodesy, Intelligence
and Mapping
Research and Development Agency
Fort Belvoir, Virginia 22060

1 Commandant
U. S. Army Command and General Staff College
Attn: Secretary
Fort Leavenworth, Kansas 66270

1 Dr. H. Robl, Deputy Chief Scientist
U. S. Army Research Office (Durham)
Box CM, Duke Station
Durham, North Carolina 27706

1 Commanding Officer
U. S. Army Research Office (Durham)
Attn: CRD-AA-IP (Richard O. Ulsh)
Box CM, Duke Station
Durham, North Carolina 27706

1 Superintendent
U. S. Army Military Academy
West Point, New York 10996

1 The Walter Reed Institute of Research
Walter Reed Medical Center
Washington, D. C. 20012

1 Commanding Officer
U. S. Army Electronics R&D Activity
Fort Huachuca, Arizona 85163

1 Commanding Officer
U. S. Army Engineer R&D Laboratory
Attn: STINFO Branch
Fort Belvoir, Virginia 22060

1 Commanding Officer
U. S. Army Electronics R&D Activity
White Sands Missile Range, New Mexico 88002

1 Dr. S. Benedict Levin, Director
Institute for Exploratory Research
U. S. Army Electronics Command
Fort Monmouth, New Jersey 07703

1 Director
Institute for Exploratory Research
U. S. Army Electronics Command
Attn: Mr. Robert O. Parker, Executive
Secretary, JSTAC (AMSEL-XL-D)
Fort Monmouth, New Jersey 07703

1 Commanding General
U. S. Army Electronics Command
Fort Monmouth, New Jersey 07703

Attn: AMSEL-SC
RD-D
RD-G
RD-GF
RD-MAF-I
RD-MAT
XL-D
XL-E
XL-C
XL-S
HL-D
HL-L
HL-J
HL-P
HL-O
HL-R
NL-D
NL-A
NL-P
NL-R
NL-S
KL-D
KL-E
KL-S
KL-T
VL-D
WL-D

3 Chief of Naval Research
Department of the Navy
Washington, D. C. 20360
Attn: Code 427

4 Chief, Bureau of Ships
Department of the Navy
Washington, D. C. 20360

3 Chief, Bureau of Weapons
Department of the Navy
Washington, D. C. 20360

2 Commanding Officer
Office of Naval Research Branch Office
Box 39, Navy No. 100 F.P.O.
New York, New York 09510

3 Commanding Officer
Office of Naval Research Branch Office
219 South Dearborn Street
Chicago, Illinois 60604

1 Commanding Officer
Office of Naval Research Branch Office
1030 East Green Street
Pasadena, California

1 Commanding Officer
Office of Naval Research Branch Office
207 West 24th Street
New York, New York 10011

Distribution list as of May 1, 1966 (cont'd.)

1 Commanding Officer
Office of Naval Research Branch Office
495 Summer Street
Boston, Massachusetts 02210

8 Director, Naval Research Laboratory
Technical Information Officer
Washington, D. C.
Attn: Code 2000

1 Commander
Naval Air Development and Material Center
Johnsville, Pennsylvania 18974

2 Librarian
U. S. Naval Electronics Laboratory
San Diego, California 95152

1 Commanding Officer and Director
U. S. Naval Underwater Sound Laboratory
Fort Trumbull
New London, Connecticut 06840

1 Librarian
U. S. Navy Post Graduate School
Monterey, California

1 Commander
U. S. Naval Air Missile Test Center
Point Magu, California

1 Director
U. S. Naval Observatory
Washington, D. C.

2 Chief of Naval Operations
OP-07
Washington, D. C.

1 Director, U. S. Naval Security Group
Attn: G43
3801 Nebraska Avenue
Washington, D. C.

2 Commanding Officer
Naval Ordnance Laboratory
White Oak, Maryland

1 Commanding Officer
Naval Ordnance Laboratory
Corona, California

1 Commanding Officer
Naval Ordnance Test Station
China Lake, California

1 Commanding Officer
Naval Avionics Facility
Indianapolis, Indiana

1 Commanding Officer
Naval Training Device Center
Orlando, Florida

1 U. S. Naval Weapons Laboratory
Dahlgren, Virginia

1 Weapons Systems Test Division
Naval Air Test Center
Patuxtent River, Maryland
Attn: Library

1 Mr. Charles F. Yost
Special Assistant to the Director of Research
National Aeronautics and Space Administration
Washington, D. C. 20546

1 Dr. H. Harrison, Code RRE
Chief, Electrophysics Branch
National Aeronautics and Space Administration
Washington, D. C. 20546

1 Goddard Space Flight Center
National Aeronautics and Space Administration
Attn: Library, Documents Section Code 252
Greenbelt, Maryland 20771

1 NASA Lewis Research Center
Attn: Library
21000 Brookpark Road
Cleveland, Ohio 44135

1 National Science Foundation
Attn: Dr. John R. Lehmann
Division of Engineering
1800 G Street, N. W.
Washington, D. C. 20550

1 U. S. Atomic Energy Commission
Division of Technical Information Extension
P. O. Box 62
Oak Ridge, Tennessee 37831

1 Los Alamos Scientific Laboratory
Attn: Reports Library
P. O. Box 1663
Los Alamos, New Mexico 87544

2 NASA Scientific & Technical Information Facility
Attn: Acquisitions Branch (S/AK/DL)
P. O. Box 33
College Park, Maryland 20740

1 Director
Research Laboratory of Electronics
Massachusetts Institute of Technology
Cambridge, Massachusetts 02139

1 Polytechnic Institute of Brooklyn
55 Johnson Street
Brooklyn, New York 11201
Attn: Mr. Jerome Fox
Research Coordinator

1 Director
Columbia Radiation Laboratory
Columbia University
538 West 120th Street
New York, New York 10027

1 Director
Coordinated Science Laboratory
University of Illinois
Urbana, Illinois 61801

1 Director
Stanford Electronics Laboratories
Stanford University
Stanford, California

1 Director
Electronics Research Laboratory
University of California
Berkeley 4, California

1 Director
Electronic Sciences Laboratory
University of Southern California
Los Angeles, California 90007

1 Professor A. A. Dougal, Director
Laboratories for Electronics and
Related Sciences Research
University of Texas
Austin, Texas 78712

1 Division of Engineering and Applied Physics
210 Pierce Hall
Harvard University
Cambridge, Massachusetts 02138

1 Aerospace Corporation
P. O. Box 95085
Los Angeles, California 90045
Attn: Library Acquisitions Group

1 Professor Nicholas George
California Institute of Technology
Pasadena, California

1 Aeronautics Library
Graduate Aeronautical Laboratories
California Institute of Technology
1201 E. California Boulevard
Pasadena, California 91109

1 Director, USAF Project RAND
Via: Air Force Liaison Office
The RAND Corporation
1700 Main Street
Santa Monica, California 90406
Attn: Library

1 The Johns Hopkins University
Applied Physics Laboratory
8621 Georgia Avenue
Silver Spring, Maryland
Attn: Boris W. Kuvshinoff
Document Librarian

1 Hunt Library
Carnegie Institute of Technology
Schenley Park
Pittsburgh, Pennsylvania 15213

1 Dr. Leo Young
Stanford Research Institute
Menlo Park, California

1 Mr. Henry L. Bachmann
Assistant Chief Engineer
Wheeler Laboratories
122 Cuttermill Road
Great Neck, New York

1 University of Liege
Electronic Department
Mathmatics Institute
15, Avenue Des Tilleuls
Val-Benoit, Liege
Belgium

1 School of Engineering Sciences
Arizona State University
Tempe, Arizona

1 University of California at Los Angeles
Department of Engineering
Los Angeles, California

1 California Institute of Technology
Pasadena, California
Attn: Documents Library

1 University of California
Santa Barbara, California
Attn: Library

1 Carnegie Institute of Technology
Electrical Engineering Department
Pittsburgh, Pennsylvania

1 University of Michigan
Electrical Engineering Department
Ann Arbor, Michigan

1 New York University
College of Engineering
New York, New York

1 Syracuse University
Department of Electrical Engineering
Syracuse, New York

1 Yale University
Engineering Department
New Haven, Connecticut

1 Airborne Instruments Laboratory
Deerpark, New York

1 Bendix Pacific Division
11600 Sherman Way
North Hollywood, California

1 General Electric Company
Research Laboratories
Schenectady, New York

1 Lockheed Aircraft Corporation
P. O. Box 504
Sunnyvale, California

1 Raytheon Company
Bedford, Massachusetts
Attn: Librarian

Security Classification

DOCUMENT CONTROL DATA R&D

(Security classification of title, body of abstract and indexing annotation must be entered when the overall report is classified)

1. ORIGINATING ACTIVITY (Corporate author) University of Illinois Coordinated Science Laboratory Urbana, Illinois 61801	2a. REPORT SECURITY CLASSIFICATION Unclassified 2b. GROUP

3. REPORT TITLE

PASSIVE DAMPING OF THE GENERAL RELATIVITY SATELLITE GYRO

4. DESCRIPTIVE NOTES (Type of report and inclusive dates)

5. AUTHOR(S) (Last name, first name, initial)

Chen, T.C. , Hsu, J. , Skaperdas, D.

6. REPORT DATE	7a TOTAL NO. OF PAGES	7b. NO. OF REFS.
November, 1966	24	12

8a. CONTRACT OR GRANT NO. DA 28 043 AMC 00073(E) b. PROJECT NO. 20014501B31F; Also in part NASA NGR 14 005 038. c. d.	9a. ORIGINATOR'S REPORT NUMBER(S) R-330 9b. OTHER REPORT NO(S) (Any other numbers that may be assigned this report)

10. AVAILABILITY/LIMITATION NOTICES

Distribution of this report is unlimited.

11. SUPPLEMENTARY NOTES	12. SPONSORING MILITARY ACTIVITY Joint Services Electronics Program thru U.S. Army Electronics Command Ft. Monmouth, New Jersey 07703

13. ABSTRACT

A passive damping method for aligning the instantaneous spin, symmetry and angular momentum axes of a solid, axially symmetric almost spherical satellite gyro is analyzed. Damping is accomplished by the dissipation of energy due to cyclic strains in the gyro body caused by its torque-free precession. Damping time is calculated for a particular gyro design.

Security Classification

KEY WORDS	LINK A ROLE	LINK A WT	LINK B ROLE	LINK B WT	LINK C ROLE	LINK C WT
Passive damping method						
Satellite gyro						

INSTRUCTIONS

1. ORIGINATING ACTIVITY: Enter the name and address of the contractor, subcontractor, grantee, Department of Defense activity or other organization (corporate author) issuing the report.

2a. REPORT SECURITY CLASSIFICATION: Enter the overall security classification of the report. Indicate whether "Restricted Data" is included. Marking is to be in accordance with appropriate security regulations.

2b. GROUP: Automatic downgrading is specified in DoD Directive 5200.10 and Armed Forces Industrial Manual. Enter the group number. Also, when applicable, show that optional markings have been used for Group 3 and Group 4 as authorized.

3. REPORT TITLE: Enter the complete report title in all capital letters. Titles in all cases should be unclassified. If a meaningful title cannot be selected without classification, show title classification in all capitals in parenthesis immediately following the title.

4. DESCRIPTIVE NOTES: If appropriate, enter the type of report, e.g., interim, progress, summary, annual, or final. Give the inclusive dates when a specific reporting period is covered.

5. AUTHOR(S): Enter the name(s) of author(s) as shown on or in the report. Enter last name, first name, middle initial. If military, show rank and branch of service. The name of the principal author is an absolute minimum requirement.

6. REPORT DATE: Enter the date of the report as day, month, year; or month, year. If more than one date appears on the report, use date of publication.

7a. TOTAL NUMBER OF PAGES: The total page count should follow normal pagination procedures, i.e., enter the number of pages containing information.

7b. NUMBER OF REFERENCES: Enter the total number of references cited in the report.

8a. CONTRACT OR GRANT NUMBER: If appropriate, enter the applicable number of the contract or grant under which the report was written.

8b, 8c, & 8d. PROJECT NUMBER: Enter the appropriate military department identification, such as project number, subproject number, system numbers, task number, etc.

9a. ORIGINATOR'S REPORT NUMBER(S): Enter the official report number by which the document will be identified and controlled by the originating activity. This number must be unique to this report.

9b. OTHER REPORT NUMBER(S): If the report has been assigned any other report numbers (either by the originator or by the sponsor), also enter this number(s).

10. AVAILABILITY/LIMITATION NOTICES: Enter any limitations on further dissemination of the report, other than those imposed by security classification, using standard statements such as:

(1) "Qualified requesters may obtain copies of this report from DDC."

(2) "Foreign announcement and dissemination of this report by DDC is not authorized."

(3) "U. S. Government agencies may obtain copies of this report directly from DDC. Other qualified DDC users shall request through
_______________________________________."

(4) "U. S. military agencies may obtain copies of this report directly from DDC. Other qualified users shall request through
_______________________________________."

(5) "All distribution of this report is controlled. Qualified DDC users shall request through
_______________________________________."

If the report has been furnished to the Office of Technical Services, Department of Commerce, for sale to the public, indicate this fact and enter the price, if known.

11. SUPPLEMENTARY NOTES: Use for additional explanatory notes.

12. SPONSORING MILITARY ACTIVITY: Enter the name of the departmental project office or laboratory sponsoring (paying for) the research and development. Include address.

13. ABSTRACT: Enter an abstract giving a brief and factual summary of the document indicative of the report, even though it may also appear elsewhere in the body of the technical report. If additional space is required, a continuation sheet shall be attached.

It is highly desirable that the abstract of classified reports be unclassified. Each paragraph of the abstract shall end with an indication of the military security classification of the information in the paragraph, represented as (TS), (S), (C), or (U).

There is no limitation on the length of the abstract. However, the suggested length is from 150 to 225 words.

14. KEY WORDS: Key words are technically meaningful terms or short phrases that characterize a report and may be used as index entries for cataloging the report. Key words must be selected so that no security classification is required. Identifiers, such as equipment model designation, trade name, military project code name, geographic location, may be used as key words but will be followed by an indication of technical context. The assignment of links, roles, and weights is optional.